Insertion of isonitrile into the Mo–C bond of $[MoCp_2(CH_3)(CNH)]^+$: a density functional study

Maria José Calhorda,[ab] Pedro E. M. Lopes[a] and Evert Jan Baerends[c]

[a] *Instituto de Tecnologia Química e Biológica (ITQB), Quinta do Marquês, EAN, Apartado 127, 2781-901 Oeiras, Portugal. E-mail: mjc@itqb.unl.pt*
[b] *Departamento de Química e Bioquímica, Faculdade de Ciências, Universidade de Lisboa, 1749-016 Lisboa, Portugal*
[c] *Scheikunding Laboratorium, Vrije Universiteit, De Boelelaan 1083, 1081HV Amsterdam, The Netherlands*

Received (in Montpellier, France) 17th January 2000, Accepted 23rd February 2000

The reaction of CNH with the methyl group in the transition metal complex $[MoCp_2(CH_3)CNH]^+$, to form a η^2-iminoacyl complex, was theoretically investigated with density functional methods. The geometries of the reactant, transition state, and product complexes were optimized at the LDA level, and then GGA single point calculations were performed on these optimized structures. The transition state for the reaction, automatically generated, has some product-like character, as the new C–C bond has partially formed, and it indicates that the mechanism consists of a methyl migration to the carbon of the isonitrile, acompanied by a reorganization of the isonitrile. The activation energy (E_a) and the reaction energy (ΔE) were calculated to be 15.9 and -14.8 kcal mol^{-1}, respectively.

Unsaturated molecules such as carbon monoxide, isocyanide, olefins, *etc.*, are able to insert into metal–hydride and metal–alkyl bonds of transition metal complexes, to form new C–H or C–C bonds, in what is a very important step, both in organic synthesis and in catalytic reactions. These reactions take place more easily and with larger yields than when only saturated groups are involved and a migration mechanism cannot operate.[1] Many experiments, involving for instance, ethylene, CO and CNR insertion reactions,[2] and theoretical studies[3,4] have been done, trying to understand these reactions, namely when one unsaturated group is involved. A relatively recent review gives a general idea of *ab initio* molecular orbital studies on catalytic elementary reactions, therefore addressing the insertion of olefins, carbonyls, and other ligands.[3a] Normally isonitriles insert more easily than carbonyls, as the resulting η^2-iminoacyl group is a more effective ligand than the η^2-acyl ligand.

In this work, we attempt to understand the mechanism of insertion of the isonitrile group in complexes $[Mo(\eta^5\text{-}C_5H_5)_2(CH_3)CNR]^+$ ($\eta^5\text{-}C_5H_5 \equiv Cp$; R, R′ = Me, Et), to form the η^2-iminoacyl complexes, as depicted in Scheme 1 for $[MoCp_2(CH_3)CNR]^+$, **1**, to give **2**. This reaction takes place overnight at room temperature or can proceed faster with thermal activation, and both complexes have been isolated and characterized.[5] Insertion reactions of this type have also been observed in the related complexes $[MoCp'(CO)_2(R)CNR]^+$ ($Cp' = \eta^5\text{-}C_5H_5$, $\eta^5\text{-}C_5Me_5$, $\eta^5\text{-}C_5H_4Me$; R = Bu^t, Pr^i, Et, Me; M = Mo, W in certain combinations) by Carmona and coworkers.[2c–f]

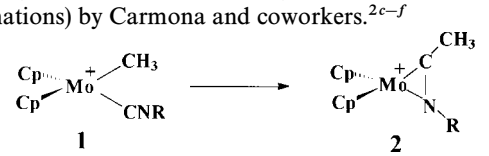

Scheme 1

Density functional methods using the ADF program[6] will be used in the theoretical calculations, aimed at determining the reaction mechanism and finding the transition state.

Experimental

DFT calculations: geometry optimizations

The density functional calculations[7] were made using the ADF package.[6] It allows the decomposition of molecules into fragments, which can be atoms or groups of atoms, making the interpretation of results easier, as concepts from qualitative MO theory can be used within the framework of a highly accurate method. This is particularly true in the area of organometallic chemistry, where numerous works are known.[8]

The basis set consisted of uncontracted Slater-type atomic orbitals. A frozen-core approximation was used, the following atomic orbitals being kept in the core: C(1s), N(1s) and Mo(1s, 2s, 2p, 3s, 3p). The basis sets used (DZ) can be described as H (double ζ, 1s), C and N (double ζ, 2s, 2p), Mo (triple ζ, 5p, 5s, 4d). All the geometry optimizations were done using the local density approximation (LDA) approach. Non local (NL) calculations including Becke's exchange corrections[9] and Perdew's nonlocal correction to the local expression of the correlation energy[10] were performed for the optimized geometries.

The geometries were based on available structures of isonitrile derivatives of molybdenocene or tungstenocene[5,11] and were idealized in order to keep the highest symmetry possible, C_s. The isonitrile was taken as CNH. The Cp rings were fixed with C–C and C–H distances of 1.39 and 1.09 Å, respectively, and each ring plane was perpendicular to the line joining the Mo atom and its center. The carbon environment in the methyl group was taken as tetrahedral, with a C–H distance of 1.10 Å. In order to optimize the geometries of the initial (**1**) and final (**2**) complexes, all the other angles and distances, including the Mo–Cp distance and the Cp–Mo–Cp angle, were allowed to vary within C_s symmetry.

DFT calculations: the transition state

Transition states are stationary points difficult to locate on the many-dimensional potential energy surface. In order to

make a search for the transition state in the reaction under study, namely the formation of the C–C bond and the coordination of the C–N group to the metal, the simpler complex $[MoCl_2(CH_3)CNH]^+$ was used to model $[MoCp_2(CH_3)CNR]^+$, that is, the Cp rings were replaced by Cl^- anions. This is a drastic approximation, but the size of the real molecule prevents its use for such a purpose. A complete grid search was therefore performed in a two-dimensional slice of the whole surface, as defined in Scheme 2.

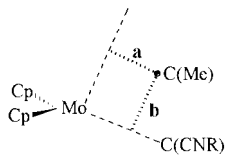

Scheme 2

For each set of *a* and *b* values within an adequate range, all other structural parameters were optimized (the internal geometry of the methyl group was kept fixed as before). This approach and the coordinate system used are the same as described by Berke and Hoffmann in their study of methyl migration into the Mn–C bond of $[Mn(CO)_5(CH_3)]$.[12] This procedure allows implicitly all mechanisms, namely insertion, migration, concerted C–C bond formation and we do not need to specify any particular mechanism. By allowing the methyl carbon to move freely on this surface, with simultaneous relaxation of all other degrees of freedom, the reaction course emerges immediately from the most favorable path on the surface. All mechanisms (alkyl migration, CNH insertion, and concerted bond formation) except radical ones are automatically considered. After construction of the three-dimensional surface and finding an approximate transition state, corresponding to the maximum energy, an automatic transition state search for the real $[MoCp_2(CH_3)CNH]^+$ complex was done.

Results

The initial and final states of the reaction

The geometries of the two Mo(IV) complexes $[MoCp_2(CH_3)CNH]^+$, **1**, and $[MoCp_2(\eta^2\text{-}(CH_3)CNH)]^+$, **2**, were optimized as described above and the final geometries are shown in Fig. 1. None of these complexes has been structurally characterized, but analogues such as $[MoCp_2(X)CNR]^+$ are known and can be used to check the quality of the results.[5,11] There are also many examples that provide evidence that the geometries calculated with density functional methods are in reasonably good agreement with experimental data.[13] In this family of compounds, the available structures are from W(IV) derivatives, but distances in Mo or W complexes are comparable. Structures were taken from the Cambridge Crystallographic Data Base.[14] In complexes $[WCp_2(Br)CNMe]Br$ and $[WCp_2(Cl)CNEt][PF_6]$, the relevant parameters are, respectively: W–C 2.03, 2.04 Å; C–N 1.17, 1.16 Å; W–Cp 1.97, 1.97 Å; Cp–W–Cp 139, 137.1°; X–W–C 83.4, 81.3°; W–C–N 179, 177.3°. These structural parameters are very different from those of the molybdenocene isonitrile derivatives, where the metal is formally Mo(II), such as $[MoCp_2(CNBu^t)]$, where the distances are Mo–C 1.997 Å; C–N 1.193 Å, and the angles are Cp–Mo–Cp 147.7°; W–C–N 139.5°.[5] The available data indicate that isonitrile bends in the more electron rich Mo(II) complex, while remaining approximately linear in the M(IV) derivatives. Therefore, in the calculated geometry for $[MoCp_2(CH_3)CNH]^+$, the structural parameters, namely Mo–C(CNH) 2.005 Å; C–N 1.184 Å; Mo–Cp 1.960 Å; C–Mo–C 80.12°, C–N–H 170.6° and Cp–Mo–Cp 140.2°, fall in the range observed for the two tungsten(IV) complexes. Finally, the Mo–C(Me) distance, calculated as 2.256 Å, is much longer than the Mo–C(CNH) bond, but very similar to the Mo–C distance in $[MoCp_2(Bu^n)_2]$, 2.268 Å.[15] The geometry obtained is always the same, whichever the starting geometry of the isonitrile, bent or linear.

The C–N bond length of 1.184 Å in **1** is much closer to a C≡N triple bond (typically 1.16 Å) than to a double bond (1.32 Å). This suggests that the CNH ligand is not acting as a strong π-acceptor, as this would lead to its bending (see discussion below).

In order to check the quality of the calculations, frequency calculations were performed. The C=N stretching frequency was determined as 2000 cm^{-1} for coordinated CNH in **1**. This compares relatively well with the experimentally obtained 2173 (s) and 2198 (sh) cm^{-1} for $[MoCp_2(Me)CNEt]^+$, 2176 (s) cm^{-1} for $[MoCp_2(Et)CNEt]^+$, 2180 (s) cm^{-1} for $[MoCp_2(Me)CNMe]^+$, and 2170 (s) cm^{-1} for $[MoCp_2(Et)CNMe]^+$, where the CNR group is linear.[5] The R and R′ groups influence the stretching frequency, so the value obtained for R = Me and R′ = H should not be exactly the same.

The optimized structure of the reaction product, $[MoCp_2(\eta^2\text{-}(CH_3)CNH)]^+$, **2**, is shown in the right side of Fig. 1 (C_s symmetry was kept during the optimization). The iminoacyl moiety is coordinated to the metal in a dihapto way, the Mo–C(CNH) distance being 2.111 Å and the new Mo–N bond 2.139 Å. The CN distance (1.265 Å) has increased significantly, when compared to the starting complex, as the formation of another bond by the N atom makes it a double bond. As no structural characterization is available, the calculated infrared stretching frequency for the C≡N bond, 1753.5 cm^{-1}, was compared and found to be in good agreement with the experimental values, 1744 (sh) cm^{-1} for $[MoCp_2(\eta^2\text{-}(Me)CNEt)]^+$, 1737 (sh) cm^{-1} for $[MoCp_2(\eta^2\text{-}(Et)CNEt)]^+$, 1750 (sh) cm^{-1} for $[MoCp_2(\eta^2\text{-}(Me)CNMe)]^+$, and 1740 (s) cm^{-1} for $[MoCp_2(\eta^2\text{-}(Et)CNMe)]^+$.[5]

These results indicate that the computed structures are very similar to the real ones, insofar as comparisons can be made. The energy of the final product **2** is lower than the energy of the starting product, showing that the reaction is exothermic ($\Delta E = -14.8$ kcal mol^{-1}).

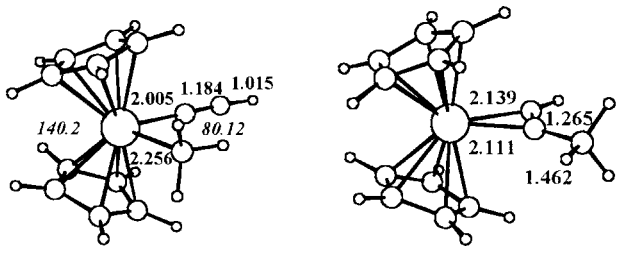

Fig. 1 Optimized geometries of the complexes in the initial and final states of the reaction, $[MoCp_2(CH_3)CNH]^+$, **1** (left), and $[MoCp_2(\eta^2\text{-}(CH_3)CNH]^+$, **2** (right).

The reaction pathway

The potential energy surface for the conversion of **1** into **2** was calculated using the simpler model $[MoCl_2(CH_3)CNH]^+$, as described above in the Experimental, and is shown in Fig. 2. Although we do not expect this simplified model to reproduce exactly the real mechanism, it should give us an approximate idea of the global changes occurring during the reaction. This was confirmed, since after defining an approximate transition state for the reaction, corresponding to the maximum in the minimum energy path, an automatic search using gradient techniques was completed successfully for the more realistic model, $[MoCp_2(CH_3)CNH]^+$. The initial geometry for the search corresponds to the maximum in the potential energy surface of the Cl^- complex, signalled as point 3 in Fig. 2.

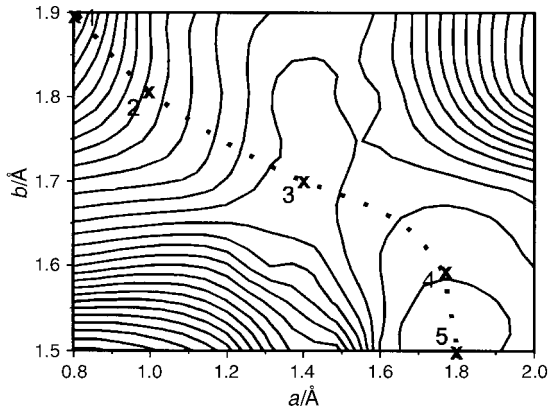

Fig. 2 Two-dimensional potential energy surface for the reaction $[MoCl_2(CH_3)CNH]^+$, **1**, to $[MoCl_2(\eta^2\text{-}(CH_3)CNH)]^+$, **2**. *a* and *b* were defined in Scheme 2 and measure the displacement of the methyl group relative to the molybdenum atom.

An internal reaction coordinate across the surface was searched and is represented in Fig. 2 by the crosses numbered 1 to 5. Point 1 represents the geometry of the starting complex $[MoCl_2(CH_3)CNH]^+$, which is slightly different from the Cp derivative, while point 5 is past the transition state, but still far from the reaction product. The geometrical changes taking place during the reaction are shown in Fig. 3.

The calculated reaction path points to a migration of the methyl group, as in the initial steps the elongation of the Mo–C(Me) bond causes little or no perturbation in the Mo–CNH unit. The Mo–C bond distance remains approximately the same (2.005 to 1.997 Å) and the Mo–C–N and C–N–H bond angles stay almost linear. The maximum in the minimum energy path (point 3) already shows some of the characteristics of the final product. The Mo–C–N angle has started to deviate from linearity (152.14°) and the same has happened to the CNH bond angle (138.01°), while the C–C distance (1.802 Å) indicates the formation of the new bond. The Mo–C and C–N bond distances are longer than in the initial complex.

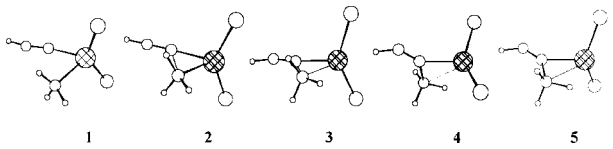

Fig. 3 Changes in geometry along the reaction for points 1–5 signalled in Fig. 2.

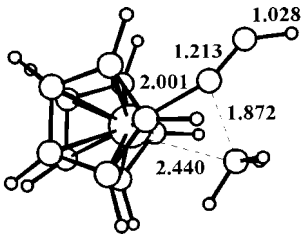

Fig. 4 The geometry of the transition state, seen from the top.

Table 1 Bonding energy decomposition for the initial complex $[MoCp_2(CH_3)CNH]^+$, **1**, the transition state (TS), and the final complex $[MoCp_2(\eta^2\text{-}(CH_3)CNH)]^+$, **2**

	1	TS	**2**
ΔE_{Pauli}	343.16	459.42	214.30
ΔE_{elec}	−517.46	−537.89	−378.06
$\boldsymbol{\Delta E_{st}}$ [a]	**−174.30**	**−78.47**	**−163.76**
ΔE_{oi} (a′)	−185.47	−272.50	−180.67
ΔE_{oi} (a″)	−30.51	−29.50	−25.30
$\boldsymbol{\Delta E_{oi}}$ [b]	**−215.98**	**−302.00**	**−205.97**
ΔE_{prep}	3.32	9.37	−32.00
$\boldsymbol{\Delta E_{tot}}$ [c]	**−386.96**	**−371.10**	**−401.73**

[a] $\Delta E_{st} = \Delta E_{Pauli} + \Delta E_{elec}$. [b] $\Delta E_{oi} = \Delta E_{oi}$ (a′) + ΔE_{oi} (a″). [c] $\Delta E_{tot} = \Delta E_{st} + \Delta E_{oi} + \Delta E_{prep}$.

The transition state

The transition state was located by performing an automatic transition state search. This corresponds to finding the normal coordinate with the only imaginary frequency, obtained from frequency calculations. To ensure that the calculated transition state represents a transformation between the desired reactant and product complexes, we examined the transition vector corresponding to the only imaginary normal frequency. The main component of the approximate reaction coordinate corresponds to the translation of the methyl group. Also important is the bending of the Mo–C–N and C–N–H bond angles.

The optimized structure of the transition state is shown in Fig. 4. The methyl group has moved towards the CNH fragment, elongating the Mo–C(Me) distance to 2.440 Å and leading to a closing of the C–Mo–C angle (48.6°). The Mo–C(CNH) bond distance, 2.001 Å, is also longer than in the starting complex.

If we compare the transition state with the maximum energy structure obtained with the $[MoCl_2(CH_3)CNH]^+$ model, we see that the real transition state has a much longer Mo–C(Me) distance, 2.440 Å compared with 2.202 Å. The C–C bond distances are very similar (1.872 and 1.802 Å) and the Mo–C–N angle is 160.4°. Both transition states are far from the product, as there is not yet a hint of the formation of the Mo–N bond, which is to be found in the final complex. Analogous transition states were found by Morokuma and coworkers[3a,4a,b] and by Dedieu and Nakamura.[16]

After the transition state, the energy falls rapidly. This corresponds to the formation of the η^2-iminoacyl complex. The decrease in energy is expected, as the Mo–C(Me) bond is already considerably weakened at the transition state, much of the distortion has taken place, and the Mo–N bond is now forming.

Energy changes along the reaction

The previous calculations of the initial complex, $[MoCp_2(CH_3)CNH]^+$, **1**, the final complex $[MoCp_2(\eta^2\text{-}(CH_3)CNH)]^+$, **2**, and the transition state enable us to obtain the relative energies.

The bonding energy decomposition scheme:

$$\Delta E = \Delta E_{prep} + \Delta E_{int}$$

where ΔE_{prep} is the energy needed to convert the separate fragments in their equilibrium geometry into fragments with the final geometry in the molecule and ΔE_{int} is the interaction energy between the prepared fragments, is used. ΔE_{int} can be further decomposed in three terms

$$\Delta E_{int} = \Delta E_{Pauli} + \Delta E_{elec} + \Delta E_{oi}$$

representing the Pauli repulsion between occupied orbitals of the fragments, the electrostatic interaction between fragments (an attractive term), and the 2-electron stabilizing interactions between occupied levels of one fragment and empty levels of the other. ΔE_{oi} can be decomposed according to the number of irreducible representations.[17]

ΔE_{prep} values were calculated as 3.05 kcal mol^{-1} for the $MoCp_2^{2+}$ fragment, 0.27 kcal mol^{-1} for the isonitrile and taken as 0 for the methyl anion, when forming

$[MoCp_2(CH_3)CNH]^+$, **1**. Another set of values was obtained for the transition state (2.56 and 6.81 kcal mol^{-1}, respectively). In the final complex, the enthalpy of formation of the ligand η^2-$(CH_3)CNR^-$ from the same fragments (CNH and methyl anion) has been calculated as -33.53 kcal mol^{-1}, while ΔE_{prep} for $MoCp_2^{2+}$ is now 1.53 kcal mol^{-1}. All the bonding energy decomposition values are collected in Table 1; the bonding will be discussed later. The energy barrier for the reaction is 15.9 kcal mol^{-1}.

A similar calculation was performed in the absence of the metal fragment. Two isolated CNH and CH_3^- fragments were allowed to approach, adopting the same geometry as in the transition state, and the reaction then continued until the iminoacyl ion was formed. Interestingly, there is no energy barrier for this reaction. We shall come back to this point later.

Discussion

The electronic structure of the initial complex

The electronic structure of $[MoCp_2(R)CNR']^+$ can be better understood by decomposing the molecule into fragments, one of them being the well known $MoCp_2^{2+}$ fragment described in detail by Lauher and Hoffmann.[18] In this d^2 Mo(IV) derivative, the lower energy a_1 orbital can be used for back donation, while the other two relevant d orbitals are empty and can receive electrons from the ligands. The other two fragments are the CNH ligand and the methyl anion, CH_3^-. The ΔE_{oi} term indicates that most interactions originate from the orbitals in the irreducible representation a′, reflecting that the three fragment orbitals mentioned above lie in the mirror plane of the molecule. The interaction diagram is depicted in Fig. 5. The frontier orbitals of CH_3^- include one carbon lone pair, the fragment "sp^3 hybrid" a_1, and a degenerate set of C–H bonding orbitals, based on C p_x and p_y orbitals, not shown. The slightly bent isonitrile has as HOMO a carbon lone pair, σ, which is responsible for the formation of the σ bond, while the π bonds may be described by the two orthogonal sets of π and π* orbitals. Only the set of orbitals in the mirror plane of the complex (defined by Mo, CNH and the carbon atom of the methyl group) interacts significantly with the metal fragment orbitals and is the only one shown in the diagram. The bending of the isonitrile leads to mixing of σ character into the π orbitals.

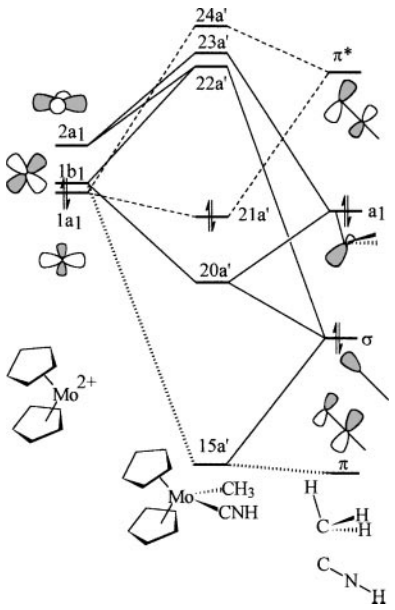

Fig. 5 Orbital interaction diagram between the $MoCp_2^{2+}$ fragment (left) and the two fragments CNH and CH_3^- (right).

The two strong σ bonds with the ligands are formed by donation from the CH_3^- lone pair a_1 and the σ orbital of the CNH ligand to the empty orbitals ($1b_1$ and $2a_1$) of $MoCp_2^{2+}$. The $1a_1$ orbital of the metallic fragment back donates to the isonitrile π*. The π orbital is also involved in the interaction, but the overlap is smaller, so that the net interaction corresponds to the isonitrile acting as a π-acceptor. Only 0.30 electrons are transferred to the π*, showing that isonitrile acts as a weak π-acceptor, in agreement with the small distortions away from linearity that were discussed above.

The electronic structure of the final complex

In the final product, the $MoCp_2^{2+}$ fragment is coordinated to the η^2-iminoacyl $CH_3C{=}NH^-$ fragment. Upon formation of the new C–C bond, the triple C≡N bond becomes a double bond, C=N, the in-plane component of the π and π* orbitals being lost. As in the initial complex, the out-of-the plane π and π* orbitals show no relevant interaction with the molybdenocene orbitals. The interaction will therefore be mainly between the ligand orbital that has a carbon lone pair character, σ, where the negative charge is mostly located, with some contribution from the nitrogen atom, and the empty $1b_1$ orbital of $MoCp_2^{2+}$. Some interaction with $2a_1$ also takes place, but the $1a_1$ orbital remains nonbonding toward the $CH_3C{=}NH^-$ fragment.

The electronic structure of the transition state

In the transition state, the C–C bond has started to form, the Mo–C(Me) bond is partially broken, and no Mo–N bond has yet formed. The decomposition into three fragments has also been adopted, in order to compare the bonding in the TS with that in the initial complex. The origin of the barrier can be traced to loss of bonding between the metal orbitals and the methyl lone pair, as a result of its reorientation, required to form the new C–C bond. Indeed, the overlap integrals between the methyl a_1 orbital and the three metal fragment orbitals have changed from 0.178, 0.032 and 0.293 in the initial complex, to 0.084, 0.299 and 0.011 in the transition state, for $1a_1$, $2a_1$ and $1b_1$, respectively. Similar effects of methyl reorientation have been described by Goddard and coworkers in the study of reductive elimination reactions and account for the increasing barrier as one moves from elimination of H_2, to CH_4, to C_2H_6.[19] The absence of barrier when the metal fragment is absent is due to the strong electrostatic attraction between the two fragments, which more than compensates the Pauli repulsion. The role of the metal fragment, therefore, can be assigned to that of a template, which holds together the two fragments and allows their subsequent reaction.

Conclusions

The reaction studied in this work can be described as a migration of the methyl group to the coordinated isonitrile, as in the transition state its bond to the metal is partially disrupted and the C–C bond is significantly formed. The presence of the metal fragment is required as a template to hold the methyl group, a small energy barrier being calculated for this exothermic reaction, in accordance with experimental findings.

Acknowledgements

We thank the HCM European network Quantum Chemistry of Transition Metal Compounds. PL acknowledges JNICT for a grant (BD 2527/RM93). MJC thanks C. C. Romão for

helpful discussions concerning the chemistry problems addressed here.

Notes and references

1 (*a*) P. M. Maitlis, H. C. Long, R. Quyoum, M. L. Turner and Z.-Q. Wang, *Chem. Comm.*, 1996, 1; (*b*) M. J. Calhorda, J. M. Brown and N. A. Cooley, *Organometallics*, 1991, **10**, 1431.

2 (*a*) F. Calderazzo, *Angew. Chem., Int. Ed. Engl.*, 1977, **16**, 299; (*b*) A. Yamamoto, *J. Chem. Soc., Dalton Trans.*, 1999, 1027; (*c*) A. Pizzano, L. Sanchéz, M. Altmann, A. Monge, C. Ruiz and E. Carmona, *J. Am. Chem. Soc.*, 1995, **117**, 1759; (*d*) M. del M. Conejo, A. Pizzano, L. Sanchéz and E. Carmona, *J. Chem. Soc., Dalton Trans.*, 1996, 3687; (*e*) J. Campora, E. Gutiérrez, A. Monge, M. L. Poveda, C. Ruiz and E. Carmona, *Organometallics*, 1993, **12**, 4025; (*f*) P. J. Daff, A. Monge, P. Palma, M. L. Poveda, C. Ruiz, P. Valerga and E. Carmona, *Organometallics*, 1997, **16**, 2263.

3 (*a*) N. Koga and K. Morokuma, *Chem. Rev.*, 1991, **91**, 823; (*b*) S. Niu, S. Zaric, C. A. Bayse, D. L. Strout and M. B. Hall, *Organometallics*, 1998, **17**, 5139; (*c*) R. Jiménez–Castaño, S. Niu and M. B. Hall, *Organometallics*, 1997, **16**, 1962; (*d*) J. Endo, N. Koga and K. Morokuma, *Organometallics*, 1993, **12**, 2777; (*e*) G. Sini, S. A. Macgregor, O. Eisenstein and J. H. Teuben, *Organometallics*, 1994, **13**, 1049; (*f*) I. Hyla–Krispin, S. Niu and R. Gleiter, *Organometallics*, 1995, **14**, 964; (*g*) T. Yoshida, N. Koga and K. Morokuma, *Organometallics*, 1995, **14**, 746; (*h*) T. Yoshida, N. Koga and K. Morokuma, *Organometallics*, 1996, **15**, 766; (*i*) T. Matsubara, N. Koga, Y. Ding, D. G. Musaev and K. Morokuma, *Organometallics*, 1997, **16**, 1065; (*j*) M. Reinhold, J. E. McGrady and R. J. Meier, *J. Chem. Soc., Dalton Trans.*, 1999, 487.

4 (*a*) S. Sakaki, K. Kitaura, K. Morokuma and K. Ohkubo, *J. Am. Chem. Soc.*, 1983, **105**, 2280; (*b*) N. Koga and K. Morokuma, *J. Am. Chem. Soc.*, 1986, **108**, 6136; (*c*) F. Hutschka, A. Dedieu and W. Leitner, *Angew. Chem., Int. Ed. Engl.*, 1995, **34**, 1742; (*d*) B. A. Markies, P. Wijkens, A. Dedieu, J. Boersma, A. L. Spek and G. van Koten, *Organometallics*, 1995, **14**, 5628; (*e*) M. Svensson, T. Matsubara and K. Morokuma, *Organometallics*, 1996, **15**, 5568.

5 A. M. Martins, M. J. Calhorda, C. C. Romão, C. Völkl, P. Kiprof and A. C. Filippou, *J. Organomet. Chem.*, 1992, **423**, 367.

6 *Amsterdam Density Functional* (*ADF*) *Program*, Vrije Universiteit, Amsterdam, The Netherlands, 1995.

7 (*a*) E. J. Baerends, D. Ellis and P. Ros, *Chem. Phys.*, 1973, **2**, 42; (*b*) E. J. Baerends and P. Ros, *Chem. Phys.*, 1973, **2**, 51; (*c*) E. J. Baerends and P. Ros, *Int. J. Quantum Chem.*, 1978, **12**, 169; (*d*) P. M. Boerrigter, G. te Velde and E. J. Baerends, *Int. J. Quantum Chem.*, 1988, **33**, 87; (*e*) G. te Velde and E. J. Baerends, *J. Comput. Phys.*, 1992, **99**, 84.

8 (*a*) T. Ziegler and A. Rauk, *Theor. Chim. Acta*, 1977, **46**, 1; (*b*) T. Ziegler and A. Rauk, *Inorg. Chem.*, 1979, **18**, 1558; (*c*) R. L. DeKock, M. A. Peterson, L. E. Reynolds, L. Chen, E. J. Baerends and P. Vernooijs, *Organometallics*, 1993, **12**, 2794; (*d*) A. Rosa and E. J. Baerends, *Inorg. Chem.*, 1992, **31**, 4717; (*e*) M. Torrent, L. Deng, M. Duran, M. Sola and T. Ziegler, *Organometallics*, 1997, **16**, 13; (*f*) L. Deng and T. Ziegler, *Organometallics*, 1996, **15**, 3011.

9 S. H. Vosko, L. Wilk and M. Nusair, *Can. J. Phys.*, 1980, **58**, 1200.

10 J. P. Perdew, J. A. Chevary, S. H. Vosko, K. A. Jackson, M. R. Pedersen, D. J. Singh and C. Fiolhais, *Phys. Rev. B: Condens. Matter*, 1992, **58**, 6671.

11 (*a*) M. J. Calhorda, A. R. Dias, M. T Duarte, A. M. Martins, P. M. Matias and C. C. Romão, *J. Organomet. Chem.*, 1992, **440**, 119; (*b*) A. C. Filippou, A. R. Dias, A. M. Martins and C. C. Romão, *J. Organomet. Chem.*, 1993, **455**, 129; A. M. Martins, PhD Thesis, Instituto Superior Técnico, Lisboa, 1991.

12 H. Berke and R. Hoffmann, *J. Am. Chem. Soc.*, 1978, **100**, 7224.

13 T. Ziegler, *Chem. Rev.*, 1991, **91**, 651.

14 F. H. Allen, J. E. Davies, J. J. Galloy, O. Johnson, O. Kennard, C. F. Macrae and D. G. Watson, *J. Chem. Inf. Comput. Sci.*, 1991, **31**, 204.

15 M. J. Calhorda, M. A. A. F. de C. T. Carrondo, A. R. Dias, A. M. Galvão, M. Helena Garcia, A. M. Martins, M. E. Minas da Piedade, C. I. Pinheiro, C. C. Romão, J. A. Martinho Simões and L. F. Veiros, *Organometallics*, 1991, **10**, 483.

16 (*a*) A. Dedieu and S. Nakamura, in *Quantum Chemistry: The Challenge of Transition Metals and Coordination Chemistry*, ed. A. Veillard, Nato ASI Series, vol. 176, Riedel, Dordrecht, 1986, p. 277; (*b*) A. Dedieu and S. Nakamura, *Chem. Phys. Lett.*, 1984, **111**, 243.

17 (*a*) T. Ziegler and A. Rauk, *Inorg. Chem.*, 1979, **18**, 1755; (*b*) T. Ziegler and A. Rauk, *Inorg. Chem.*, 1979, **18**, 1758; (*c*) T. Ziegler and A. Rauk, *Theor. Chim. Acta*, 1977, **46**, 1.

18 J. W. Lauher and R. Hoffmann, *J. Am. Chem. Soc.*, 1976, **98**, 1729.

19 (*a*) J. J. Low and W. A. Goddard III, *J. Am. Chem. Soc.*, 1984, **106**, 6928; (*b*) J. J. Low and W. A. Goddard III, *J. Am. Chem. Soc.*, 1984, **106**, 8321; (*c*) J. J. Low and W. A. Goddard III, *Organometallics*, 1986, **5**, 609; (*d*) J. J. Low and W. A. Goddard III, *J. Am. Chem. Soc.*, 1986, **108**, 6115; (*e*) E. A. Carter and W. A. Goddard, *J. Am. Chem. Soc.*, 1987, **109**, 579.